DNA Vaccination via RALA Nanoparticles in a Microneedle Delivery System Induces a Potent Immune Response against the Endogenous Prostate Cancer Stem Cell Antigen

Grace Cole[2], Ahlam A. Ali[1], Emma McErlean[1], Eoghan J Mulholland, Amy Short, Cian M. McCrudden[1], Joanne McCaffrey[3], Tracy Robson[4], Vicky L. Kett[1], Jonathan A. Coulter[1], Nicholas J. Dunne[5], Ryan F. Donnelly[1], Helen O. McCarthy[1]*

*Corresponding Author

[1]School of Pharmacy, Queen's University Belfast, Belfast BT9 7BL, Northern Ireland, UK

[2]Department of Pathology, University of British Columbia, BC V5T 2B5, Canada

[3]Department of Pharmacology and Therapeutics, University College Cork, Cork T12 YN60, Ireland

[4]Molecular & Cellular Therapeutics, Royal College of Surgeons in Ireland, Dublin 2, Ireland

[5]School of Mechanical and Manufacturing Engineering, Dublin City University, Dublin 9, Ireland

Email: h.mccarthy@qub.ac.uk

Tel.: +44 02890 972149
Fax: +44 02890 247794

Abstract

Castrate resistant prostate cancer (CRPC) remains a major challenge for healthcare professionals. Immunotherapeutic approaches, including DNA vaccination, hold the potential to harness the host's own immune system to mount a cell-mediated, anti-tumour response, capable of clearing disseminated tumour deposits. These anti-cancer vaccines represent a promising strategy for patients with advanced disease, however, to date DNA vaccines have demonstrated limited efficacy in clinical trials, owing to the lack of a suitable DNA delivery system. This study was designed to evaluate the efficacy of a two-tier delivery system incorporating cationic RALA/pDNA nanoparticles (NPs) into a dissolvable microneedle (MN) patch for the purposes of DNA vaccination against prostate cancer. Application of NP-loaded MN patches successfully resulted in endogenous production of the encoded prostate stem cell antigen (PSCA). Furthermore, immunisation with RALA/pPSCA loaded MNs elicited a tumour-specific immune response against TRAMP C-1 tumours *ex vivo*. Finally, vaccination with RALA/pPSCA loaded MNs demonstrated anti-tumour activity in both prophylactic and therapeutic prostate cancer models in vivo. This is further evidence that this two-tier MN delivery system is a robust platform for prostate cancer DNA vaccination.

Key Words: DNA Vaccine; Microneedle; PSCA; RALA; CTL; Nanoparticle; Prostate Cancer

1. Introduction

As the second leading cause of cancer-related deaths of males within the UK, prostate cancer represents a major challenge to healthcare professionals.[1] There is no available cure for metastatic or castrate resistant disease, and therefore efficacious, new treatments are urgently required.[2] Within the past couple of decades there has been growing interest in anti-cancer vaccines which harness the body's immune system to target cells expressing immunogenic tumour-associated antigens (TAAs).[3] Of these, DNA vaccines provide a relatively simple and effective means of inducing a cellular immune response against encoded TAAs.[3] However, despite producing promising results in preclinical studies, prostate cancer DNA vaccines have demonstrated mixed efficacy in clinical trials.[3] Further to this, the recent failure of PROSTVAC™ (Bavarian Nordic, US) to achieve the primary outcome measure of increasing overall survival in a Phase III clinical trial for men with asymptomatic or minimally symptomatic mCRPC has raised doubts about the efficacy of DNA vaccines as a monotherapy.[4] Thus there is a need to develop novel DNA delivery systems to improve the efficacy of such vaccines.

To develop a clinically relevant prostate cancer DNA vaccine several key issues need to be considered including the choice of target antigen. Numerous immunogenic proteins are expressed nearly exclusively by the prostate or malignant prostate tissue, providing multiple potential targets for immunotherapy. One TAA is the Prostate Stem Cell Antigen (PSCA),[5] a GPI-anchored cell surface antigen expressed in normal and malignant prostate tissue.[5] PSCA expression correlates with prostate cancer grade and stage, and 94% of primary prostate tumours (105/112), and 100% of secondary bone metastases (9/9) express PSCA, making it a particularly strong target for advanced diseased.[6] As well as being expressed by humans, a murine homologue of PSCA has been identified,[7] and the establishment of mPSCA-expressing murine prostate cancer cell lines from transgenic mice has provided a physiologically relevant model to study the anti-tumour efficacy of prostate cancer DNA vaccines.[7,8]

Apart from the TAA of choice, the effectiveness of a DNA vaccine is also dictated by the success of the delivery system. As such, microneedles (MNs) represent an ideal delivery platform for DNA vaccination purposes, as these micro-projections localise the genetic cargo across the stratum corneum (SC) to a rich network of antigen-presenting cells (APCs) in the dermis and epidermis.[9] The transfection of APCs and subsequent display of antigenic peptides on Major Histocompatibility Complex (MHC) I and II molecules is central to the

stimulation and expansion of TAA-specific CD8+ and CD4+ T cells, the effectors of the adaptive immune system.[3] Additionally, this physical delivery approach can easily be combined with a vector-based strategy to enhance cellular uptake within this highly immunogenic area. Previously, a two-tier delivery system immunised mice against the HPV-16 E6 and E7 cervical cancer TAAs using nanoparticles (NP) loaded into a polymeric MN. Immunisation via the NP-MN delivery platform resulted in tumour retardation in both prophylactic and therapeutic tumour models,[11,][10] but was limited by a low delivery dose and poor compatibility of the NP cargo within the PVP matrix. Thorough screening of a range of polymers to form the MN matrix and lyophilising NPs prior to MN formation has increased both the functionality and the loading of NP cargo within the polymer matrix.[11,12] In this investigation, the NP-MN platform was employed to immunise mice with encoded mPSCA, and it was reported for the first time for prostate cancer DNA vaccination. Application of the NP-MN system successfully resulted in local mPSCA expression within the treated ears of mice. Furthermore, immunisation of mice with the NP-MN system induced a tumour-specific cellular immune response, and inhibited the growth of TRAMP C-1 tumours in both prophylactic and therapeutic challenge models.

Materials and Methods

2.1 Preparation of RALA/pPSCA Nanoparticles (NP) and Lipofectamine/pPSCA NPs

The RALA peptide (WEARLARALARALARHLARALARALRACEA) was supplied as a lyophilised powder from Biomatik Corporation (USA). The powder was stored at -20^{o}C and reconstituted in DNase/RNase free water (Life Technologies, UK) for experimentation. A plasmid encoding the murine prostate TAA, PSCA (pPSCA), was purchased from Origene (USA) within the pCMV-AC-GFP expression vector, resulting in expression of PSCA with a C-terminal turbo-GFP tag to allow visualisation and quantification of successful transfection. pPSCA was transformed and propagated in *Escherichia coli* DH5α cells (Life Technologies, UK) as per manufacturer's instructions. The plasmid was isolated and purified using PureLink HiPure Plasmid Filter Maxiprep Kits (Life Technologies, UK) prior to use.

RALA/pPSCA nanoparticles (NP) were formed at various N:P ratios as described previously.[13] Briefly, the desired quantity of plasmid was added to DNase/RNase free water, prior to addition of the desired quantity of RALA solution. NPs were left for 30 min at room temperature (RT) prior to experimentation to ensure complete complexation.

Lipofectamine 2000 was purchased from Thermofischer Scientific (UK) as a positive control. Lipofectamine/pPSCA lipoplexes were formed as per the manufacturer's instructions. Briefly, 3 µg of pPSCA and 6 µL of Lipofectamine 2000 were conditioned separately in 150 µL of Opti-MEM media for 5 min at RT, and subsequently mixed together and allowed to incubate for a further 5 min prior to use.

2.2 Lyophilisation protocol for NPs

To produce lyophilised NPs (L-NPs), NP solutions containing 5% w/v Trehalose were placed into a VirTis Wizard 2.0 (SP Scientific, USA) and subjected to freezing at -40^{o}C for 1 h, before primary drying for 3 h at -35^{o}C (120 mTorr), -30^{o}C for 4 h (190 mTorr) and -25^{o}C for 4 h (190 mTorr). Finally, samples underwent secondary drying for 18 h at 20^{o}C (190 mTorr for 8 h and 50 mTorr for 10 h).

2.3 Gel Retardation Assay

RALA/pPSCA complexes were prepared at N:P ratios 0.25 - 12 using 1 µg of pDNA in a total volume of 20 µL. 10 µL of sample was supplemented with 2 µL 5X Nucleic Acid Loading Buffer (Bio-Rad, USA), and loaded on to a 1% Agarose gel incorporating 0.2 µg/mL EtBr as a DNA intercalating agent. Samples were electrophoresed at 100 V for 1 h in 1X TAE buffer and then visualised under UV light using a Multispectrum Bioimaging System (UVP, UK).

2.4 Picogreen Encapsulation Assay

RALA/pPSCA complexes were prepared at N:P ratios 0.5 - 12 using 1 µg of pDNA in a total volume of 1000 µL DNase/RNase free water. 50 µL samples were added to black 96 well plates in triplicate and supplemented with 50 µL Quanti-iT Picogreen reagent. Samples were left to incubate for 30 min at RT prior to quantification of fluorescent emission at 520 nm using a Synergy 2 Multi-Mode Microplate Reader (BioTek Instruments Inc, UK) following excitation at 480 nm. The percentage of encapsulated pPSCA was calculated relative to the fluorescence of a pDNA only sample.

2.5 Size and Zeta Potential Analysis of RALA/pPSCA complexes

RALA/pPSCA complexes were prepared for N:P ratios 1-15, in a volume of 50 µL DNase/RNase free water. The hydrodynamic size and zeta potential of complexes was determined using a Malvern Zetasizer NanoZS (Malvern Instrument Ltd, UK) via Dynamic Light Scattering and Laser Doppler Velocimetry respectively. For stability studies, NPs were

prepared at N:P 10, and incubated at RT for up to 28 days prior to analysis. For temperature stability studies the hydrodynamic size of NPs was determined over an increasing temperature range from 4-37^{o}C.

2.6 Transmission Electron Microscopy (TEM)

NPs (N:P 10) were prepared using 1 µg of pPSCA in a total volume of 30 µL. Samples were coated on to Carbon coated Cu grids (Taab Laboratories Equipment Ltd, UK) by placing the grid face down on to a 10 µL NP solution for 10 min. The grid was then dried overnight and stained the following day with UranyLess electromicroscopy stain (Electron Microscopy Services, USA) for 2 min prior to rinsing with distilled water and drying at RT. The grid was then imaged using a JEM-1440Plus TEM (Joel, USA) at an accelerating voltage of 120 kV.

2.7 Serum Stability Study

NPs (N:P 10) were prepared using 1 µg of pPSCA in a total volume of 50 µL. Samples were incubated alone or with 10% Foetal Calf Serum (FCS) at 37^{o}C for 1-6 h. Samples were subsequently either untreated or incubated with 5 µL of 10% Sodium Dodecyl Sulphate (SDS) for 10 min at RT to dissociate NPs and free pPSCA. 20 µL samples were subsequently electrophoresed and visualised on an agarose as described in Section 2.3.

2.8 Cell Culture

The immortalised murine dendritic cell line, DC 2.4, was maintained in RPMI media supplemented with 10% FCS, 1% L-glutamine, 1% HEPES and 1% Non Essential Amino Acids (Life Technologies, UK). The human epithelial Human Embryonic Kidney 293 (HEK-293) cell line was maintained in DMEM supplemented with 10% FCS (Life Technologies, UK). The murine prostate cancer cell line, Transgenic adenocarcinoma Mouse Prostate Cell Line 1 (TRAMP C-1), was maintained in DMEM, adjusted to contain 4mM L-glutamine, 1.5 g/L sodium bicarbonate and 4.5 g/L glucose (ATCC, USA), supplemented with 0.005 mg/mL Bovine Insulin, 10 nM Dehydroisoandrosterone (Sigma, UK), 5% FCS (Life Technologies, UK) and 5% Nu-Serum IV (VWR, UK). For *ex vivo* experimentation TRAMP C-1 media was further supplemented with 1% Penicillin/Streptomycin (Life Technologies, UK).

2.9 Transfection studies

For cytotoxicity studies HEK-293 and DC 2.4 cells were seeded into 96 well plates at densities of 15,000 and 20,000 cells/well respectively and left to adhere overnight. Prior to transfection

cells were conditioned for 2 h in Opti-MEM (Life Technologies, UK). Cells were then supplemented with 0.5 µg/well pPSCA complexed to RALA (N:P 0-12) for 6 h before being replaced in complete media. 24 h following transfection, cells were supplemented with 10% CellTiter 96 Aqueous One Solution Reagent (MTS) (Promega, UK) for 2 h, and the absorbance at 490 nm was subsequently measured using an EL808 96-well plate reader (BioTek Instruments Inc, UK). The percentage viability was determined relative to untreated controls.

For transfection studies HEK-293 and DC 2.4 cells were seeded into 6 well plates at densities of 300,000 and 400,000 cells/well respectively and left to adhere overnight. Cells were conditioned and treated as above with 3 µg/well pPSCA complexed to RALA (N:P 0-12). For polymerase chain reaction (PCR) experiments, cells were transfected as above with freshly prepared RALA NPs (N:P 10), Lipofectamine/pPSCA, or with L-NPs (N:P 10) which had been reconstituted in 20% w/w 9-10 kDa PVA solution (Sigma, UK), dried overnight in non-indented silicon moulds and dissolved in Opti-MEM prior to transfection.

For quantification of GFP expression, cells were harvested in 4% Formaldehyde (Sigma, UK) 48 h post-transfection and GFP expression was quantified via flow cytometry using a BD Accuri C6 Plus Flow Cytometer (BD Biosciences, UK). Data was analysed using the machine's in-built software and fluorescent intensity is reported at 4% gating to untreated cells.

For determination of PSCA expression via amplification PCR, cells were harvested in TRIzol reagent (Thermofischer Scientific, UK) and mRNA was extracted as per the manufacturer's instructions. Prior to RT-PCR reactions, mRNA was treated to remove any contaminating pDNA from samples using the DNase I, RNase-free kit (Thermofischer Scientfic, UK) as per the manufacturer's instructions. 1000 ng of mRNA was then reverse transcribed to cDNA by supplementing samples with 10 µL of Reverse Transcription mix (4 µL 5X First Strand Buffer, 1 µL 10 mM dNTP mix, 1 µL Dilute Random Primer, 2 µL 0.1 M DTT, 1 µL RNase OUT 40U/mL, 1 µL M-MLV Reverse Transcriptase, [Invitrogen, UK]) and heating to 25^{o}C for 5 min, 37^{o}C for 90 min, and 70^{o}C for 10 min, before cooling to 4^{o}C in a TC-312 Thermocycler (Bibby Scientific Ltd, UK). Following reverse transcription, 3 µL of cDNA sample was transferred to a fresh RNase-free PCR tubes with 11 µL of PCR Mastermix, containing forward (5'-CTG GCC ACC TAC TTA GCC CT-3') and reverse (5'-GCG ATG TAA AGC AAC TGT GC-3') primers for the murine PSCA (mPSCA) gene. PSCA was amplified via PCR using the following conditions: Initial denaturation at 95^{o}C for 2 min, followed by 30 cycles of amplification at 95^{o}C for 1 min, 57^{o}C for 1 min and 72^{o}C for 1 min, and a final extension period

of 5 min at 72°C. Following amplification, samples were electrophoresed and visualised on a 2% Agarose gel as per Section 2.4. mRNA from TRAMP C-1 cells was harvested and amplified as above to serve as a positive control for mPSCA expression, while untreated cells were harvested and amplified to serve as a negative control for gene expression.

2.10 Microneedle (MN) manufacture

Microneedles were manufactured as previously described.[12] Briefly, L-NPs (N:P 10), containing 100 µg of pPSCA, were reconstituted in 30 mg of 20% w/w 9-10 kDa PVA solution and mixed manually until a homogenous solution was formed. The solution was then transferred to a silicon microneedle (MN) master-mould containing 361 inverted conical projections with dimensions of 300 µm diameter and 600 µm length, spaced 50 µm apart.[14] The solution was centrifuged at 4,000 rpm for 5 min to fill the conical indents with NP-PVA solution, following which 500 mg of inert 20% w/w 9-10 kDa PVA solution was added to the mould and re-centrifuged to form a baseplate. MNs were left to dry for 48 h at RT before carefully peeling from the mould and removal of excess baseplate and sidewalls with scalpel.

2.11 Determination of mPSCA expression *in vivo*

All *in vivo* experiments were compliant with the UK Scientific Act 1986, and carried out under project license 2794. Experimental procedures utilised male C57 BL/6 mice (Charles River, UK) 6-8 weeks old which were housed at 21°C and 50% humidity, and given unlimited access to food and water. NP loaded MNs were applied to the left ears (LE) of anaesthetised male C57 BL/6 mice for 5 min using manual pressure, and adhered in place for a further 24 h using 3M surgical tape (Micropore Ltd, UK). Right ears (RE) were left untreated to serve as a negative control. 24 h following MN removal mice were sacrificed, ears were harvested and placed into RNALater solution (Sigma, UK) for 24 h at RT. Samples were then stored at -80°C until thawed for mRNA extraction. For mRNA extraction, samples were placed into Round-Bottomed 2.0 mL Safe-Lock Eppendorf containing 500 µL of TRIzol Reagent and two 7 mm Stainless Steel beads (Qiagen, UK). Samples were homogenised in a TissueLyser LT (Qiagen, UK) using and oscillation rate of 50 osc/sec for 10 min. Following homogenisation, the mRNA extraction procedure and subsequent determination of mPSCA expression via amplification PCR followed the procedure outlined in section 2.9.

2.12 Immunisation Schedule

C57 BL/6 were immunised with approximately 100 µg of pPSCA and received a total of 3 immunisations, two weeks apart. Immunisation was either with naked pPSCA via i.m. injection (DNA-IM), naked pPSCA via MN (DNA-MN), NP via i.m. injection (NP-IM) or NP-loaded MN (NP-MN). For i.m. injections mice received a single injection into the medial thigh muscle with cargo which had been lyophilised and reconstituted in 50 µL sterile water. For MN treatment mice were immunised with two MNs (one on each ear), which were applied as previously described,[12] and have previously been demonstrated to deliver approximately 50 µg of pDNA per patch.[12]

2.13 Quantification of IFN-γ secretion

13 days following the third immunisation, prior to splenocyte harvest, TRAMP C-1 cells were plated into 24 well plates at densities of 50,000 cells/well and allowed to adhere overnight. The following morning cells were irradiated for 5 min using a 160 kVp x-ray source (Faxitron X-ray, USA) with a 0.8 mm filter, to serve as a source of re-stimulation for PSCA-specific T cells. 14 days following the third immunisation, mice were sacrificed and the spleens were aseptically harvested, mechanically homogenised and resuspended in Red Blood Cell Lysing Buffer Hybri-Max (Sigma Aldrich, Uk) for 5 min at RT to allow lysis of red blood cells within the splenocyte mixture. Cells were subsequently co-cultured at a ratio of 50:1 with irradiated TRAMP C-1 cells for up to 6 days in the presence of 20 units of murine interleukin-2 (mIL-2) (Peprotech, UK) at 37^{o}C. To allow discernment of baseline levels of cell lysis, T cells from control mice were also incubated without the presence of irradiated TRAMP C-1 cells. 4 days following re-stimulation in the presence of irradiated TRAMP C-1 cells, the supernatant from cells was harvested and IFN-γ within the supernatant was quantified via sandwich ELISA, using the Murine IFN-γ Standard ABTS ELISA Development Kit (Peprotech, UK) as per the manufacturer's instructions.

2.14 LDH Cytotoxicity Assay

14 days following the third immunisation, the spleen from each mouse was isolated, processed and stimulated as above. 6 days following re-stimulation viable T cells were harvested and resuspended in 1% BSA assay medium. Cells were incubated 10:1 with viable TRAMP C-1 cells which had been seeded at a density of 10,000 cells/well in a 96 well plate the previous day. Following 5 h incubation at 37^{o}C, the supernatant from each well was collected and the

cell specific TRAMP C-1 lysis was determined by measuring the Lactate dehydrogenase (LDH) release from damaged cells, using a Cytotoxicity Detection Kit [LDH] (Roche, UK).

2.15 Prophylactic Tumour Challenge Study

C57 BL/6 mice (N=6 or 7) underwent immunisation as in section 2.12. 14 days following the third immunisation, mice were challenged with a s.c. injection of $5x10^6$ TRAMP C-1 cells suspended in a PBS/Matrigel (BD Bioscience, UK) mixture, into the left flank. Mice were monitored for tumour growth by palpation, and measuring three times weekly. Tumour volume was calculated using the following formula: $V = \frac{4}{3}\pi r^3$. Experimental endpoint was reached when tumours attained a geometric mean diameter (GMD) of 10, or 100 days following tumour challenge. Humane endpoint was reached when mice lost <20% of their body weight, tumours became ulcerated, or mice developed persistent or severe ill health (poor conditioning, appearance, gait).

2.16 Therapeutic Tumour Challenge Study

C57 BL/6 mice (N=5/6) were challenged with a s.c. injection of $5x10^6$ TRAMP C-1 cells suspended in a PBS/Matrigel (BD Bioscience, UK) mixture, into the left flank. 7 days following implantation, when tumours had reached a palpable size (~2 mm), mice were immunised as in section 2.12. Tumour development was measured three times weekly using callipers and tumour volume was calculated as in section 2.15. Experimental endpoint was reached when tumours attained a GMD of 12, or 100 days following tumour challenge. Humane endpoint was reached when mice lost <20% of their body weight, tumours became ulcerated, or mice developed persistent or severe ill health (poor conditioning, appearance, gait).

2.17 Statistical Analysis

Unless otherwise stated experiments have three independent replicates and are expressed as mean ± standard error mean (SEM). Unless otherwise stated statistical differences were analysed using a One-Way ANOVA with a P value ≤ 0.05 considered significant.

3. Results

3.1 Physiochemical Characterisation and stability of RALA/pPSCA NPs

Gel retardation analysis indicated that RALA encapsulated free pPSCA from an N:P ratio of 2 onwards, as shown by the inability of pPSCA to migrate through an agarose gel under current

from an N:P ratio of 2 onwards (Figure 1-A). This was further supported by the PicoGreen encapsulation assay which indicated that at an N:P ratio of 0.5, 70.93% ± 10.27 of pPSCA was free in solution and able to bind PicoGreen, and that at N:P 1 the amount of free pDNA had decreased to 37.97% ± 13.31, this was then further reduced to <10% of pPSCA being free to bind PicoGreen from an N:P ≥ 2 (Figure 1-B). However, size and charge analysis revealed that RALA did not complex plasmid into cationic NPs until an N:P ratio ≥ 3 (Figure 1-C). This is due to the nearly neutral charge of complexes at N:P 2, which results in large aggregates due to a lack of charge repulsion. At N:P ≥ 4 NP mean hydrodynamic sizes were consistently <100 nm and ranged from 47.27 – 93.09 nm, with mean complex zeta potentials ranged from 4.534 – 13.57 mV.

NPs were stable over a 28 day incubation period at RT, with no significant differences in hydrodynamic size or zeta potential being observed ($p > 0.05$, Figure 2-A). We did note an increase in particle size at Day 14, with a correspondingly lower zeta potential, although this was not significant. This is not typical for RALA-NPs, as previous studies have demonstrated that the size of RALA NPs has remained < 100 nm consistently for up to 30 days.[10,15] NP hydrodynamic size also remained stable over a range of temperatures from 4-37^{o}C (Figure 2-B). Finally, the stability of pPSCA within NPs was tested via serum stability (Figure 3-B). NPs protected pPSCA from degradation by serum nucleases for up to 6 h at 37^{o}C in the presence of FCS.

3.2 *In vitro* assessment of RALA/pPSCA NPs

The effect of RALA/pPSCA NPs on the viability of HEK-293 and DC 2.4 cells was assessed using the MTS assay. With both cell lines there was a trend that transfecting cells with increasing N:P ratios resulted in decreasing cell viabilities, however, over the range of NP ratios examined (N:P 0-12) no significant decrease in cell viability was observed in either cell line (Figure 3-A).

Flow cytometry was used to evaluate the percentage of HEK-293 and DC 2.4 cells producing GFP-tagged mPSCA following transfection at varying N:P ratios (Figure 3-B). Analysis revealed that complexing pPSCA to RALA resulted in significantly higher transfection efficacies at N:P ratios ≥ 4 and ≥ 10, in HEK-293 cells and DC 2.4 cells respectively, compared to using naked pPSCA (N:P 0) alone.

As well as quantifying protein production via flow cytometry, the production of mPSCA within transfected HEK-293 (Figure 3-Ci) and DC 2.4 cells (Figure 3-Cii) was verified using end point

RT-PCR. Amplification of cDNA from untreated TRAMP C-1 cells, with mouse specific PSCA primers generated a cDNA band of the expected 130 bp size. Expression of mPSCA was not detected in untreated HEK-293 and DC 2.4 cells, as determined by a lack of visible cDNA band following amplification of cDNA. Conversely, amplification of cDNA from HEK-293 and DC 2.4 cells transfected with freshly prepared RALA/pPSCA NPs and Lipofectamine/pPSCA NPs resulted in generation of cDNA bands of the expected size, indicating successful mPSCA mRNA production following transfection.

To demonstrate that RALA/pPSCA NPs remained functional following the MN manufacturing process, cells were also transfected with L-NPs which had been dried in 9-10 kDa PVA solution (Figure 3-D). As above, amplification of cDNA harvested from untreated HEK-293 and DC 2.4 cells did not generate a gene expression product, however, cDNA harvested from HEK-293 and DC 2.4 cells following transfection yielded a 130 bp product indicating the presence of mPSCA. Therefore, it can be concluded that NPs remain functional following lyophilisation and incorporation into 9-10 kDa PVA gels.

3.3 RALA/pPSCA-MN (NP-MN) application generates gene expression *in vivo* and elicits an antigen-specific immune response

Prior to using NP-MNs for immunisation of mice, it was established that NP-MN application to the back of mouse ears generated local expression of the antigenic mPSCA. mPSCA was detected via end point RT-PCR within the left ears of mice following NP-MN application, but not in the untreated right ears of mice, indicating that gene expression was confined to the local area of MN application (Figure 4-B).

IFN-γ and cytotoxicity assays were carried out to examine the antigen-specific cell-mediated immune response following immunisation. The presence of IFN-γ in the supernatant of T cell-enriched splenocytes from immunised and naive mice, following stimulation with irradiated TRAMP C-1 cells was determined using quantitative sandwich ELISA (Figure 4-C). Immunisation with NP-MN resulted in increased secretion of IFN-γ from stimulated T cell-enriched splenocytes compared to naive mice. However, increased levels of IFN-γ secretion into the supernatant were not detected from splenocytes harvested from mice immunised with DNA-MN. The results indicate that immunisation of mice with RALA/pPSCA NPs results in a greater release of IFN-γ from splenocytes in response to stimulation with tumour cells, consistent with a PSCA-specific T_{H1}-predominant response.

The cytolytic activity of splenic T cells, from immunised and untreated control mice, against TRAMP C-1 tumour cells was then assessed using the LDH release assay (Figure 4-D). Splenic T cells from mice immunised with NP-MN (21.91%, $p < 0.05$) lysed significantly greater numbers of TRAMP C-1 cells when co-cultured at a ratio of 10:1 than those from naive mice (7.36%), indicating a robust cytotoxic immune response following NP immunisation. Conversely, immunisation of mice with pPSCA alone did not result in a significant increase in the TRAMP C-1 specific CD8+ T cell population compared to control (12.02%, $p > 0.05$).

3.4 NP-MN Immunisation delays tumour uptake and slows tumour progression in a prophylactic prostate cancer model

In the prophylactic challenge model, following tumour implantation mice were monitored three times weekly for the formation of palpable tumours (Figure 5-B). Mice receiving no immunisation (control) had all developed palpable tumours 7 days following implantation. However, immunisation with DNA-IM, DNA-MN and NP-IM delayed time until tumour development, with an average time to tumour development of 11.17, 7.57 and 11.17 days respectively. The greatest delays in tumour development were observed in mice immunised with NP-MN, where the average time to tumour formation was 16.2 days. Furthermore, 100 days following immunisation with NP-MN 1 mouse remained tumour-free, indicating that immunisation with NP-MN was able to delay, and in some cases prevent, tumour development.

Immunisation of mice with NP-MN was also able to significantly lower the tumour burden compared to control (unimmunised mice) (Figure 5-C -, Two-Way ANOVA, $p < 0.05$). For example, at 70 days post-challenge control mice had an average tumour volume of 393.8 mm^3, whilst mice immunised with NP-MN, had an average tumour volume of 124.8 mm^3.

Furthermore, immunisation with NP-MN was able to significantly extend survival of mice compared to control (Figure 5-D, $p < 0.05$, Mantel-Cox Test). Indeed, 2/6 mice immunised via NP-MN survived greater than 100 days post-challenge, (1 other mouse was censored at day 75 due to the development of a non-healing ulcer prior to experimental end-point).

3.5 NP-MN Immunisation delays tumour progression and improves survival in a therapeutic prostate cancer model

In the therapeutic challenge model immunisation with NP-MN was able to significantly lower the tumour burden compared to control (Figure 6-B, Two-Way ANOVA, $p < 0.05$). For example, at day 63 following tumour challenge, the average tumour volume of mice immunised

with NP-MN was 347.7 mm^3, whilst control mice, and mice immunised with DNA-MN, DNA-IM and NP-IM had average tumour volumes of 589.9, 544.5, 478.5 and 493.7 mm^3 respectively (Figure 6-B). Additionally, immunisation with NP-MN was able to significantly extend the survival of mice by ~10 days compared to control (81.33 vs 71 days respectively) (Figure 6-C, $p < 0.05$, Mantel-Cox Test).

4. Discussion

It has been demonstrated for the first time that MNs may be used to enhance the therapeutic efficacy of DNA vaccines targeting PSCA in a murine model of prostate cancer. In order to be successful in the clinic, DNA vaccines must overcome the barriers to gene delivery to generate sufficient TAA expression *in vivo* to elicit the expansion of an antigen-specific T cell response. This delivery of pTAA is thought to be the main stumbling block for many DNA vaccines due to the vulnerability of pDNA to degradation along with a reduced capacity to transfect cells independently. To this end non-viral vectors which are capable of simultaneously masking the anionic charge of pDNA, complexing pDNA into the NP size range and mediating cellular uptake are being developed.[16] To be efficacious *in vivo,* vectors must retain these characteristics at body temperature, and protect pDNA from degradation via serum nucleases.[17–20] Therefore the first aim of this study was to determine that complexing pPSCA to the RALA delivery peptide resulted in NPs with ideal properties for mediating transfection. The RALA peptide has previously been demonstrated to form nanoscale complexes with pDNA, which are stable at RT, resistant to degradation within the serum, and enhance transfection efficacy *in vitro* and *in vivo*.[13] Here complexation of pPSCA with RALA also resulted in NPs with ideal physical properties for cellular uptake. Furthermore, NPs were stable at body temperature, and were able to protect pPSCA from degradation for up to 6 h within serum. Therefore the functionality of RALA/pPSCA NPs was confirmed *in vitro* utilising HEK-293 cells (as a model human cell line for transfection studies),[21] and DC 2.4 cells (as DCs are an abundant cell line within the skin and are the key activators of potent cellular immune responses).[22–24] As expected, flow cytometric and PCR analysis confirmed that complexing pDNA to RALA resulted in significantly increased gene expression within both cell lines.

In addition to ensuring sufficient cellular uptake following delivery, the cargo delivery site is of key importance to DNA vaccine efficacy. Central to the induction of an adaptive immune response is the priming, stimulation and subsequent expansion of an effector population of

antigen-specific T cells. This process is reliant on the presentation of antigenic peptides by APCs on MHC class I and II molecules, to CD8+ and CD4+ T cells respectively, either following direct transfection or capture of antigenic peptide produced by bystander cells.[3] Given the fundamental role of APCs in DNA vaccination, it is illogical that the majority of DNA vaccines targeting prostate cancer are delivered i.m. or s.c. clinically,[3] where there is a relative paucity of APCs, and this may help to explain the limited efficacy of these therapies to date. A more rational approach is targeting cargo to the skin, which harbours a high density of "professional" APCs including specialised DCs which are adept at T cell priming. [23,25,26] Previously, we reported the development of a novel two-tier NP-MN delivery platform, which was able to induce a greater immune response to the encoded cargo than delivering the same cargo via i.m. injection.[12] By utilising lyophilisation to concentrate NPs prior to incorporation into the dissolvable PVA MN matrix we were able to load 57 μg of pDNA into one device, of which 50 μg was able to be delivered over a 24 h period *in vivo*. Despite undergoing the repeated concentration and drying steps of lyophilisation and MN manufacture, NPs released from the device retained a high (75%) bioactivity compared to fresh NPs, making the device ideal for delivery of high quantities of pDNA intradermally, which has been difficult to achieve previously.[27] The NP-MN device was able to penetrate neonatal porcine skin and withstand the mechanical forces needed for manual application, and perhaps more importantly was able to retain mechanical robustness and cargo functionality over a 28 day period, indicating that the device was ideal for DNA vaccination purposes.[12] Therefore, having established the functionality of RALA/pPSCA NPs, the L-NPs were incorporated into MNs to target gene expression to the epidermal and dermal layers of the skin which are abundant in specialised APCs. Lyophilisation and incorporation into the dissolvable PVA matrix did not compromise the ability of NPs to transfect the human epithelial or murine DC lines, and hence NPs released from dissolvable PVA MNs were expected to be capable of eliciting PSCA expression *in vivo*. Prior to utilising NP-MNs for immunisation studies, it was confirmed that the platform was capable of generating gene expression within the ear pinna of mice, which was selected as the site of immunisation due to the relative low density of hair follicles (which compromise MN penetration) and high abundance of APCs.[28] Application of NP-loaded MNs for 24 h resulted in antigen expression within the treated area, and so this is expected to result in antigen presentation via DCs to naive CD8+ and CD4+ T cells, generating an anti-mPSCA response.

Having established the ability of the delivery system to induce antigen expression *in vivo,* the activation of an antigen-specific T cell response was evaluated. Central to the induction of a potent, anti-tumour response is the generation of tumour-specific cytotoxic T lymphocytes (CTLs) which are capable of directly lysing cancer cells. Cytotoxic T cell responses are also heavily dependent on CD4+ T helper cells, and so anti-tumour immunity requires simultaneous expansion of an antigen-specific T_{H1} CD4+ T cell population, to stimulate CD8+ T cells.[29–31] IFN-γ secretion from the splenocytes of vaccinated animals was assessed to determine the induction of a T_{H1} response. IFN-γ is a proinflammatory cytokine released from activated DCs, CD4+ T_{H1} cells and CD8+ T cells in response to antigenic stimulation, and is critical for tumour control through the activation of macrophages and neutrophils, which contribute to tumour clearance, and the activation of CTLs.[30,32,33] As such, the greater release of IFN-γ from splenocytes of mice vaccinated with both NP-NP and NP-IM indicated the induction of an antigen-specific T_{H1}-predominant response. Additionally, the cytolytic activity of tumour-specific CTLs from vaccinated animals was demonstrated via measurement of TRAMP C-1 tumour cell lysis *in vitro*.

Given that the induction of PSCA-specific CD4+ T_{H1} and CD8+ T cells has been correlated previously with increased survival of tumour bearing mice,[34–36] and both NP-IM and NP-MN elicited antigen-specific T cells responses, it was expected that immunisation of mice with NP-MN or NP-IM injection would confer protection against C57 BL/6 mice against tumour challenge. This would also be in agreement with our previous studies which demonstrated that immunisation with both NP-MN and NP-IM could increase survival of tumour-bearing mice in a cervical cancer model.[12] Indeed in the prophylactic arm of the tumour challenge studies, immunisation with NP-MN resulted in increased time until tumour uptake (with 1/6 mice not developing a tumour) and prolonged survival of tumour-bearing mice. However, surprisingly, immunisation of mice with IM injection was only able to delay time until tumour uptake, and was not sufficient to increase survival. Previously, Johnson *et al* (2007) had reported that as many as 6 i.d. immunisations with a plasmid expressing rat PAP (pTVG-RP) were necessary to generate an anti-PAP response in Lewis rats,[37] therefore a higher number of immunisations may be needed to prevent tumour uptake in all vaccinated animals. Alternatively, the superior efficacy of the NP MN system may be due to the differing release kinetics of the NPs from the MN system which may produce a more persistent immune response. Chen *et al* (2013) demonstrated that sustained release of peptide antigen from a depot of embeddable chitosan needles elicited a stronger antibody response against the model antigen

than the same dose delivered by i.m. injection.[38] This response persisted for at least 6 weeks, and was in agreement with other studies establishing that the slower release of antigen could increase the longevity and potency of the immune response. [39,40] Correspondingly, in the therapeutic arm of the tumour challenge studies, immunisation with NP-MN significantly retarded the growth of established tumours, and prolonged survival. These results were unexpected given that immunisation via both MN and IM injection were capable of generating increased numbers of antigen-specific CTLs, which were capable of lysing TRAMP C-1 target cells *ex vivo*. A key reason for this disparity may be the time taken for each of the immunisation routes to prime CD4+ and CD8+ T cells. Indeed the high APC population in the mouse ear pinna, and the drainage of these cells to a common lymph node may facilitate faster T cell priming.[28]

An alternative explanation for the lack of efficacy of the NP-IM treatment arm may be that although CTLs are generated following immunisation, they are unable to overcome the mechanisms of immune evasion employed by the established tumour. These mechanisms include the downregulation of MHC complex presentation, immune-editing, immune suppression via regulatory T cells, secretion of immunosuppressive cytokines, and upregulation of co-inhibitory signalling pathways.[41,42] These mechanisms also likely contributed to NP-MN immunisation only modestly retarding the growth of PSCA-expressing tumours *in vivo*, indicating that this vaccination platform is insufficient to induce tumour regression in isolation. This is perhaps because most prostate cancer DNA vaccines are delivered simultaneously with adjuvants to skew the immune response,[3] and hence the platform's efficacy is likely to be improved significantly from combination with immune-modulating therapies in future studies. Several strategies have been successfully employed to counteract the escape mechanisms of the tumour microenvironment, including the use of multivalent strategies,[43] monoclonal antibodies targeting regulatory T cells,[44] adjuvants to skew the immune response,[34] and checkpoint inhibitors.[44] Given the complexity and heterogeneity of the tumour microenvironment a combination of these approaches is likely to be needed simultaneously to DNA vaccine therapy to achieve a synergistic effect yielding clinically meaningful results. One of the key advantages of DNA vaccines is that they carry the potential to encode multiple biological cargos within the same plasmid backbone. Therefore, multiple immunogenic peptides, biological adjuvants, and monoclonal antibodies could be simultaneously generated from one cost-effective and stable platform, giving this device great adaptability for future studies.

In conclusion, it has been successfully demonstrated for the first time that cutaneous administration of DNA vaccine via microneedles is capable of eliciting an immune response towards an endogenous prostate cancer TAA. Furthermore, NP-MN immunisation was able to protect against challenge with a syngeneic prostate cancer allograft, in both prophylactic and therapeutic studies. The ability of the NP-MN immunisation to generate a tumour-specific CTL response in the absence of additional adjuvants is encouraging, and the amenability of this platform to combination with other anti-cancer strategies makes it a promising candidate for future studies.

Acknowledgements

This research was supported by a Prostate Cancer UK Award (S12-006).

Statement of Significance

This research explains the development and utilisation of our unique microneedle (MN) DNA delivery system, which enables penetration through the *stratum corneum* and deposition within the highly immunogenic skin layers via a dissolvable MN matrix, and facilitates cellular uptake via complexation of pDNA cargo into nanoparticles (NPs) with the RALA delivery peptide. We report for the first time on using the NP-MN platform to immunise mice with encoded Prostate Stem Cell Antigen (mPSCA) for prostate cancer DNA vaccination. Application of the NP-MN system resulted in local mPSCA expression in vivo. Furthermore, immunisation with the NP-MN system induced a tumour-specific cellular immune response, and inhibited the growth of TRAMP C-1 prostate tumours in both prophylactic and therapeutic challenge models in vivo.

References

[1] Office of National Statistics, Cancer registration statistics, England - Office for National Statistics, (2016). https://www.ons.gov.uk/peoplepopulationandcommunity/healthandsocialcare/conditionsanddiseases/bulletins/cancerregistrationstatisticsengland/final2016 (accessed January 20, 2019).

[2] E. David Crawford, C.S. Higano, N.D. Shore, M. Hussaink, D.P. Petrylak{, Treating Patients with Metastatic Castration Resistant Prostate Cancer: A Comprehensive

Review of Available Therapies, J. Urol. 194 (2015) 1537–1547. doi:10.1016/j.juro.2015.06.106.

[3] G. Cole, J. McCaffrey, A.A. Ali, H.O. McCarthy, DNA vaccination for prostate cancer: Key concepts and considerations, Cancer Nanotechnol. 6 (2015). doi:10.1186/s12645-015-0010-5.

[4] N. (Medscape) Mulcahy, Futile: Prostate Cancer Vaccine Phase 3 Trial Ends, Medscape. (2017). https://www.medscape.com/viewarticle/885877 (accessed April 11, 2018).

[5] R.E. Reiter, Z. Gu, T. Watabe, G. Thomas, K. Szigeti, E. Davis, M. Wahl, S. Nisitani, J. Yamashiro, M.M. Le Beau, M. Loda, O.N. Witte, Prostate stem cell antigen: a cell surface marker overexpressed in prostate cancer., Proc. Natl. Acad. Sci. U. S. A. 95 (1998) 1735–40. http://www.pubmedcentral.nih.gov/articlerender.fcgi?artid=19171&tool=pmcentrez&rendertype=abstract (accessed April 17, 2016).

[6] Z. Gu, G. Thomas, J. Yamashiro, I.P. Shintaku, F. Dorey, A. Raitano, O.N. Witte, J.W. Said, Prostate stem cell antigen (PSCA) expression increases with high gleason score , advanced stage and bone metastasis in prostate cancer, (2000) 1288–1296.

[7] D. Yang, G.E. Holt, M.P. Velders, E.D. Kwon, W.M. Kast, Murine Six-Transmembrane Epithelial Antigen of the Prostate, Prostate Stem Cell Antigen, and Prostate-specific Membrane Antigen: Prostate-specific Cell-Surface Antigens Highly Expressed in Prostate Cancer of Transgenic Adenocarcinoma Mouse Prostate Mice, Cancer Res. 61 (2001) 5857–5860. http://cancerres.aacrjournals.org/content/61/15/5857.short (accessed January 4, 2015).

[8] B. a Foster, J.R. Gingrich, E.D. Kwon, C. Madias, N.M. Greenberg, Characterization of Prostatic Epithelial Cell Lines Derived from Transgenic Adenocarcinoma of the Mouse Prostate (TRAMP) Model Advances in Brief Characterization of Prostatic Epithelial Cell Lines Derived from Transgenic Adenocarcinoma of the Mouse Pros, (1997) 3325–3330.

[9] J. McCaffrey, R.F. Donnelly, H.O. McCarthy, Microneedles: an innovative platform for gene delivery., Drug Deliv. Transl. Res. 5 (2015) 424–37. doi:10.1007/s13346-015-0243-1.

572 [10] A.A. Ali, C.M. McCrudden, J. McCaffrey, J.W. McBride, G. Cole, N.J. Dunne, T.
573 Robson, A. Kissenpfennig, R.F. Donnelly, H.O. McCarthy, DNA vaccination for
574 cervical cancer; a novel technology platform of RALA mediated gene delivery via
575 polymeric microneedles, Nanomedicine Nanotechnology, Biol. Med. 13 (2017).
576 doi:10.1016/j.nano.2016.11.019.

577 [11] G. Cole, J. McCaffrey, A.A. Ali, J.W. McBride, C.M. McCrudden, E.M. Vincente-
578 Perez, R.F. Donnelly, H.O. McCarthy, Dissolving microneedles for DNA vaccination:
579 Improving functionality via polymer characterization and RALA complexation, Hum.
580 Vaccines Immunother. 13 (2017). doi:10.1080/21645515.2016.1248008.

581 [12] G. Cole, A.A. Ali, C.M. McCrudden, J.W. McBride, J. McCaffrey, T. Robson, V.L.
582 Kett, N.J. Dunne, R.F. Donnelly, H.O. McCarthy, DNA vaccination for cervical
583 cancer: Strategic optimisation of RALA mediated gene delivery from a biodegradable
584 microneedle system, Eur. J. Pharm. Biopharm. 127 (2018) 288–297.
585 doi:10.1016/J.EJPB.2018.02.029.

586 [13] H.O. Mccarthy, J. McCaffrey, C.M. Mccrudden, A. Zholobenko, A.A. Ali, J.W.
587 McBride, A.S. Massey, S. Pentlavalli, K.-H. Chen, G. Cole, S.P. Loughran, N.J.
588 Dunne, R.F. Donnelly, V.L. Kett, T. Robson, Development and characterization of
589 self-assembling nanoparticles using a bio-inspired amphipathic peptide for gene
590 delivery, J. Control. Release. 189 (2014). doi:10.1016/j.jconrel.2014.06.048.

591 [14] R.F. Donnelly, R. Majithiya, T.R.R. Singh, D.I.J. Morrow, M.J. Garland, Y.K. Demir,
592 K. Migalska, E. Ryan, D. Gillen, C.J. Scott, A.D. Woolfson, Design, optimization and
593 characterisation of polymeric microneedle arrays prepared by a novel laser-based
594 micromoulding technique., Pharm. Res. 28 (2011) 41–57. doi:10.1007/s11095-010-
595 0169-8.

596 [15] J. McCaffrey, C.M. McCrudden, A.A. Ali, A.S. Massey, J.W. McBride, M.T.C.
597 McCrudden, E.M. Vicente-Perez, J.A. Coulter, T. Robson, R.F. Donnelly, H.O.
598 McCarthy, Transcending epithelial and intracellular biological barriers; A prototype
599 DNA Delivery device, J. Control. Release. (2016). doi:10.1016/j.jconrel.2016.02.023.

600 [16] M. Ramamoorth, A. Narvekar, Non viral vectors in gene therapy- an overview., J.
601 Clin. Diagn. Res. 9 (2015) GE01-6. doi:10.7860/JCDR/2015/10443.5394.

602 [17] K. Kawabata, Y. Takakura, M. Hashida, The fate of plasmid DNA after intravenous

injection in mice: involvement of scavenger receptors in its hepatic uptake., Pharm. Res. 12 (1995) 825–30. http://www.ncbi.nlm.nih.gov/pubmed/7667185 (accessed December 30, 2015).

[18] N. Nayerossadat, T. Maedeh, P.A. Ali, Viral and nonviral delivery systems for gene delivery., Adv. Biomed. Res. 1 (2012) 27. doi:10.4103/2277-9175.98152.

[19] H.O. McCarthy, Y. Wang, S.S. Mangipudi, A. Hatefi, Advances with the use of bio-inspired vectors towards creation of artificial viruses., Expert Opin. Drug Deliv. 7 (2010) 497–512. doi:10.1517/17425240903579989.

[20] S.P. Loughran, C.M. McCrudden, H.O. McCarthy, Designer peptide delivery systems for gene therapy, Eur. J. Nanomedicine. 7 (2015) 85–96. doi:10.1515/ejnm-2014-0037.

[21] P. Thomas, T.G. Smart, HEK293 cell line: a vehicle for the expression of recombinant proteins., J. Pharmacol. Toxicol. Methods. 51 (n.d.) 187–200. doi:10.1016/j.vascn.2004.08.014.

[22] K. Palucka, J. Banchereau, Cancer immunotherapy via dendritic cells., Nat. Rev. Cancer. 12 (2012) 265–77. doi:10.1038/nrc3258.

[23] A. Stoecklinger, T.D. Eticha, M. Mesdaghi, A. Kissenpfennig, B. Malissen, J. Thalhamer, P. Hammerl, Langerin+ dermal dendritic cells are critical for CD8+ T cell activation and IgH γ-1 class switching in response to gene gun vaccines., J. Immunol. 186 (2011) 1377–83. doi:10.4049/jimmunol.1002557.

[24] K.J. Farrand, N. Dickgreber, P. Stoitzner, F. Ronchese, T.R. Petersen, I.F. Hermans, Langerin+ CD8alpha+ dendritic cells are critical for cross-priming and IL-12 production in response to systemic antigens., J. Immunol. 183 (2009) 7732–42. doi:10.4049/jimmunol.0902707.

[25] P. Stoitzner, M. Zanella, U. Ortner, M. Lukas, A. Tagwerker, K. Janke, M.B. Lutz, G. Schuler, B. Echtenacher, B. Ryffel, F. Koch, N. Romani, Migration of langerhans cells and dermal dendritic cells in skin organ cultures: augmentation by TNF-alpha and IL-1beta., J. Leukoc. Biol. 66 (1999) 462–70. http://www.ncbi.nlm.nih.gov/pubmed/10496317 (accessed February 11, 2016).

[26] J. Valladeau, S. Saeland, Cutaneous dendritic cells., Semin. Immunol. 17 (2005) 273–83. doi:10.1016/j.smim.2005.05.009.

[27] E. Gonzalez-Gonzalez, T.J. Speaker, R.P. Hickerson, R. Spitler, M.A. Flores, D. Leake, C.H. Contag, R.L. Kaspar, Silencing of reporter gene expression in skin using siRNAs and expression of plasmid DNA delivered by a soluble protrusion array device (PAD)., Mol. Ther. 18 (2010) 1667–74. doi:10.1038/mt.2010.126.

[28] P. Förg, P. von Hoegen, W. Dalemans, V. Schirrmacher, Superiority of the ear pinna over muscle tissue as site for DNA vaccination, Gene Ther. 5 (1998) 789–797. doi:10.1038/sj.gt.3300628.

[29] M.D.L.L. Garcia-Hernandez, A. Gray, B. Hubby, W.M. Kast, In vivo effects of vaccination with six-transmembrane epithelial antigen of the prostate: A candidate antigen for treating prostate cancer, Cancer Res. 67 (2007) 1344–1351. doi:10.1158/0008-5472.CAN-06-2996.

[30] R. Kennedy, E. Celis, Multiple roles for CD4+ T cells in anti-tumor immune responses., Immunol. Rev. 222 (2008) 129–44. doi:10.1111/j.1600-065X.2008.00616.x.

[31] K.L. Knutson, M.L. Disis, Tumor antigen-specific T helper cells in cancer immunity and immunotherapy., Cancer Immunol. Immunother. 54 (2005) 721–8. doi:10.1007/s00262-004-0653-2.

[32] O.A.W. Haabeth, A.A. Tveita, M. Fauskanger, F. Schjesvold, K.B. Lorvik, P.O. Hofgaard, H. Omholt, L.A. Munthe, Z. Dembic, A. Corthay, B. Bogen, How Do CD4(+) T Cells Detect and Eliminate Tumor Cells That Either Lack or Express MHC Class II Molecules?, Front. Immunol. 5 (2014) 174. doi:10.3389/fimmu.2014.00174.

[33] Y.-P. Lai, C.-J. Jeng, S.-C. Chen, The roles of CD4+ T Cells in tumor immunity, ISRN Immunol. 2011 (2011) 1–6. doi:10.5402/2011/497397.

[34] X. Zhang, C. Yu, J. Zhao, L. Fu, S. Yi, S. Liu, T. Yu, W. Chen, Vaccination with a DNA vaccine based on human PSCA and HSP70 adjuvant enhances the antigen-specific CD8+ T-cell response and inhibits the PSCA+ tumors growth in mice., J. Gene Med. 9 (2007) 715–26. doi:10.1002/jgm.1067.

[35] M.D.L.L. Garcia-Hernandez, A. Gray, B. Hubby, O.J. Klinger, W.M. Kast, Prostate stem cell antigen vaccination induces a long-term protective immune response against prostate cancer in the absence of autoimmunity., Cancer Res. 68 (2008) 861–9.

663 doi:10.1158/0008-5472.CAN-07-0445.

664 [36] K. Zhang, F. Yang, J. Ye, M. Jiang, Y. Liu, F. Jin, Y. Wu, A novel DNA/peptide
665 combined vaccine induces PSCA-specific cytotoxic T-lymphocyte responses and
666 suppresses tumor growth in experimental prostate cancer., Urology. 79 (2012)
667 1410.e7-13. doi:10.1016/j.urology.2012.02.011.

668 [37] L.E. Johnson, T.P. Frye, N. Chinnasamy, D. Chinnasamy, D.G. McNeel, Plasmid
669 DNA vaccine encoding prostatic acid phosphatase is effective in eliciting autologous
670 antigen-specific CD8+ T cells., Cancer Immunol. Immunother. 56 (2007) 885–95.
671 doi:10.1007/s00262-006-0241-8.

672 [38] L. Guo, J. Chen, Y. Qiu, S. Zhang, B. Xu, Y. Gao, Enhanced transcutaneous
673 immunization via dissolving microneedle array loaded with liposome encapsulated
674 antigen and adjuvant., Int. J. Pharm. 447 (2013) 22–30.
675 doi:10.1016/j.ijpharm.2013.02.006.

676 [39] E.C. Ehman, G.B. Johnson, J.E. Villanueva-meyer, S. Cha, A.P. Leynes, P. Eric, Z.
677 Larson, T.A. Hope, Role of sustained antigen release from nanoparticle vaccines in
678 shaping the T cell memory phenotype, 46 (2017) 1247–1262.
679 doi:10.1002/jmri.25711.PET/MRI.

680 [40] Y. Umeki, M. Saito, Y. Takahashi, Y. Takakura, M. Nishikawa, Retardation of
681 Antigen Release from DNA Hydrogel Using Cholesterol-Modified DNA for Increased
682 Antigen-Specific Immune Response, Adv. Healthc. Mater. 6 (2017) 1–8.
683 doi:10.1002/adhm.201700355.

684 [41] D.S. Vinay, E.P. Ryan, G. Pawelec, W.H. Talib, J. Stagg, E. Elkord, T. Lichtor, W.K.
685 Decker, R.L. Whelan, H.M.C.S. Kumara, E. Signori, K. Honoki, A.G. Georgakilas, A.
686 Amin, W.G. Helferich, C.S. Boosani, G. Guha, M.R. Ciriolo, S. Chen, S.I.
687 Mohammed, A.S. Azmi, W.N. Keith, A. Bilsland, D. Bhakta, D. Halicka, H. Fujii, K.
688 Aquilano, S.S. Ashraf, S. Nowsheen, X. Yang, B.K. Choi, B.S. Kwon, Immune
689 evasion in cancer: Mechanistic basis and therapeutic strategies., Semin. Cancer Biol.
690 35 Suppl (2015) S185-98. doi:10.1016/j.semcancer.2015.03.004.

691 [42] A. Thakur, U. Vaishampayan, L.G. Lum, Immunotherapy and immune evasion in
692 prostate cancer., Cancers (Basel). 5 (2013) 569–90. doi:10.3390/cancers5020569.

[43] M. Krupa, M. Canamero, C.E. Gomez, J.L. Najera, J. Gil, M. Esteban, Immunization with recombinant DNA and modified vaccinia virus Ankara (MVA) vectors delivering PSCA and STEAP1 antigens inhibits prostate cancer progression, Vaccine. 29 (2011) 1504–1513. doi:10.1016/j.vaccine.2010.12.016.

[44] W. Xue, R.L. Metheringham, V.A. Brentville, B. Gunn, P. Symonds, H. Yagita, J.M. Ramage, L.G. Durrant, W. Xue, R.L. Metheringham, V.A. Brentville, P. Symonds, H. Yagita, J.M. Ramage, L.G.D. Scib, R.L. Metheringham, A. Victoria, B. Gunn, P. Symonds, H. Yagita, J.M. Ramage, G. Durrant, SCIB2 , an antibody DNA vaccine encoding NY- ESO-1 epitopes , induces potent antitumor immunity which is further enhanced by checkpoint blockade, Oncoimmunology. 5 (2016) 1–13. doi:10.1080/2162402X.2016.1169353.

720

721 **FIGURES**

722

723

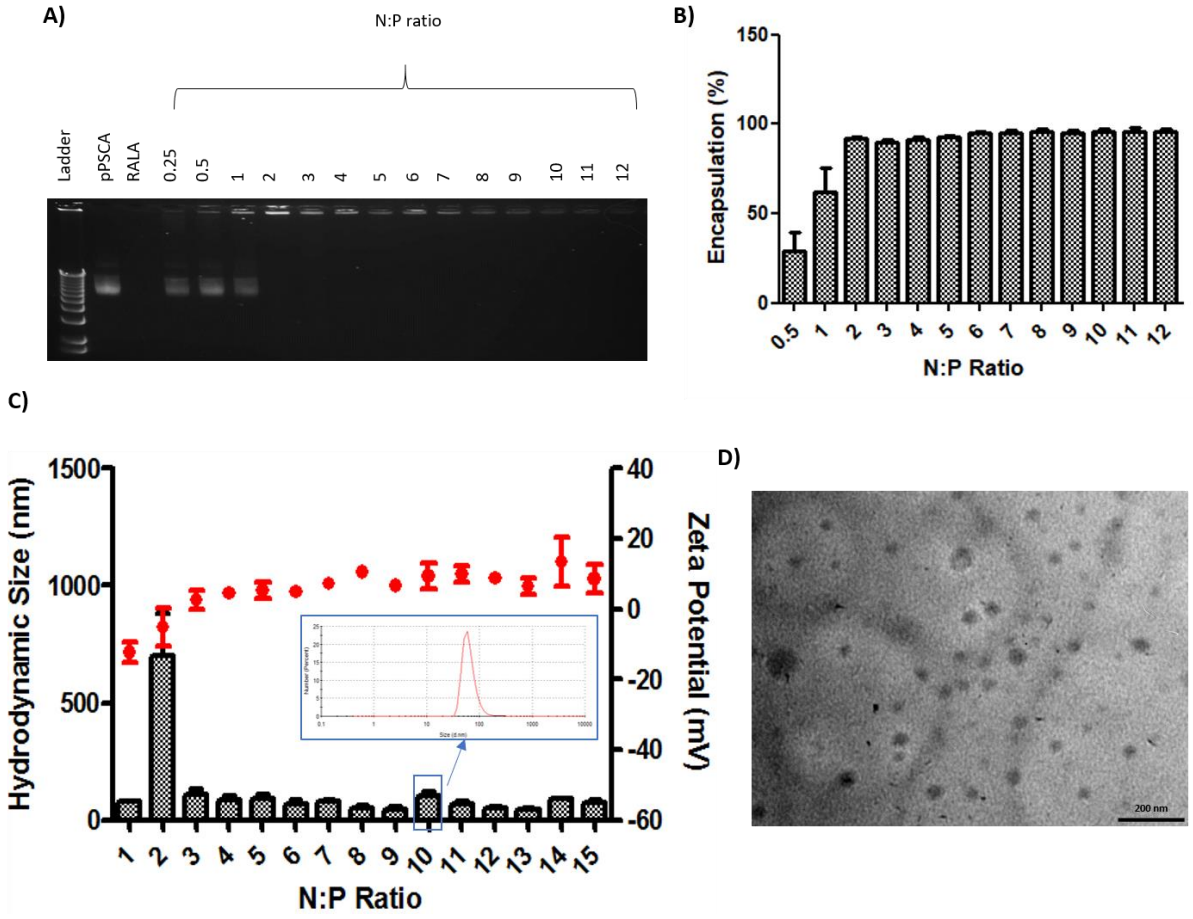

724

725

726 **Figure 1: Physiochemical characteristics of RALA/pPSCA Nanoparticles (NPs).** (A) Gel Retardation
727 Assay of NPs over a range of N:P ratios (N:P 0-12), Lane 1: DNA Ladder; Lane 2: pTAA only; Lane 3:
728 RALA only Lanes 4-17: RALA/pPSCA complexes prepared at N:P ratios 0.25-12; (B) Picogreen
729 Encapsulation Assay of NPs over a range of N:P ratios (0-12); (C) Size and Zeta Potential of NPs over a
730 range of N:P ratios (0-15), with an inlaid Size Distribution by Number graph of NPs prepared at N:P 10;
731 (D) TEM image of RALA/pPSCA NP (N:P 10), scale bar is 200 nm.

732

733

734

735

736

737

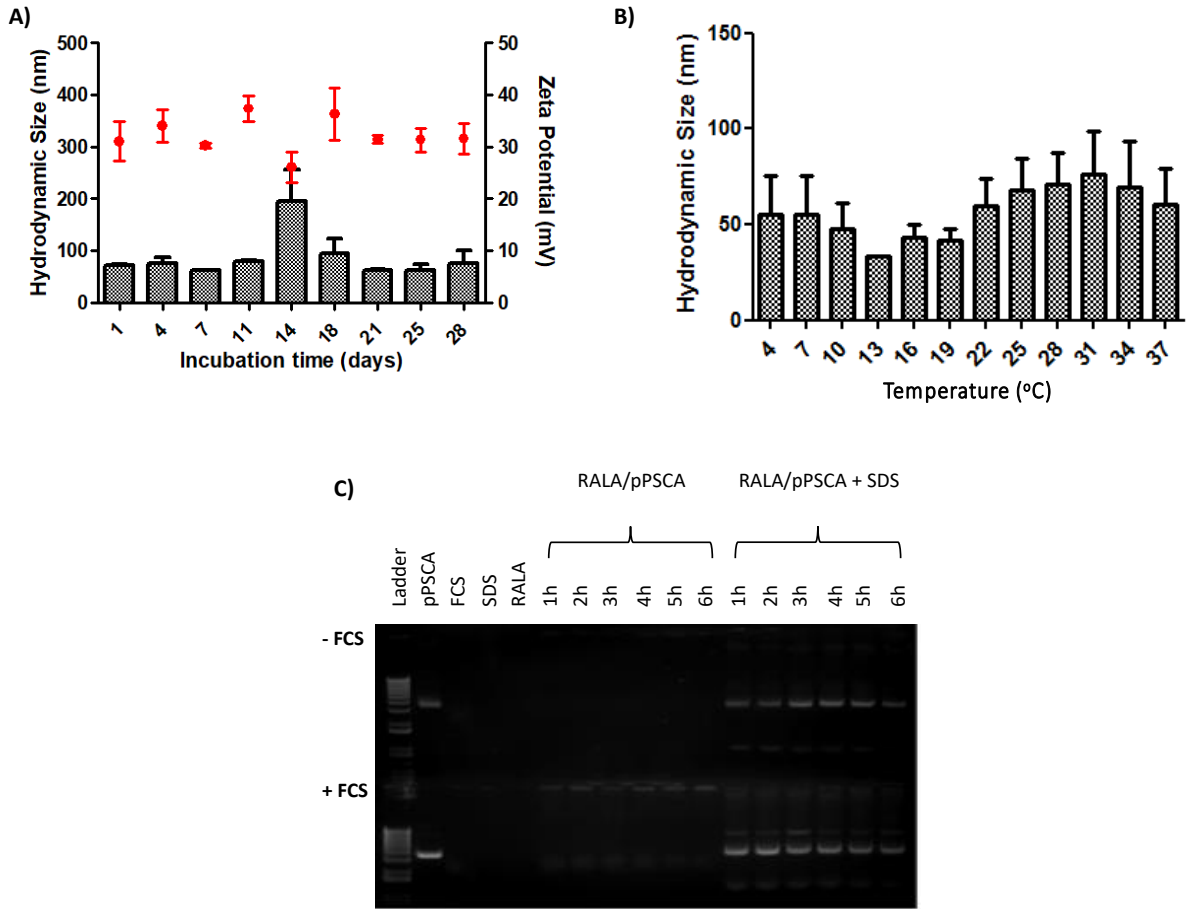

738

739

740

741

742 **Figure 2: Stability of RALA/pPSCA Nanoparticles (NPs).** (A) Hydrodynamic size and Size of
743 RALA/pPSCA NPs (N:P 10) over time. (B) Hydrodynamic Size and PDI of RALA/pPSCA NPs (N:P 10) over
744 range of temperatures (4°C - 37°C); (C) Serum Stability study of RALA/pPSCA NPs. Lane 1: DNA Ladder;
745 Lane 2: pPSCA only; Lane 3: Foetal Calf Serum (FCS); Lane 4: SDS; Lane 5: RALA peptide; Lanes 6-11:
746 RALA/pPSCA (N:P 10) and incubated in water (Row 1) or 10% FCS (Row 2) for 1-6 h at 37°C; Lanes 12-
747 17: RALA/pPSCA (N:P 10) were incubated in water (Row 1) or 10% FCS (Row 2) for 1-6 h at 37°C, and
748 subsequently decomplexed with 10% SDS for 10 min at room temperature prior to electrophoresis.

749

750

751

752

753

754

755

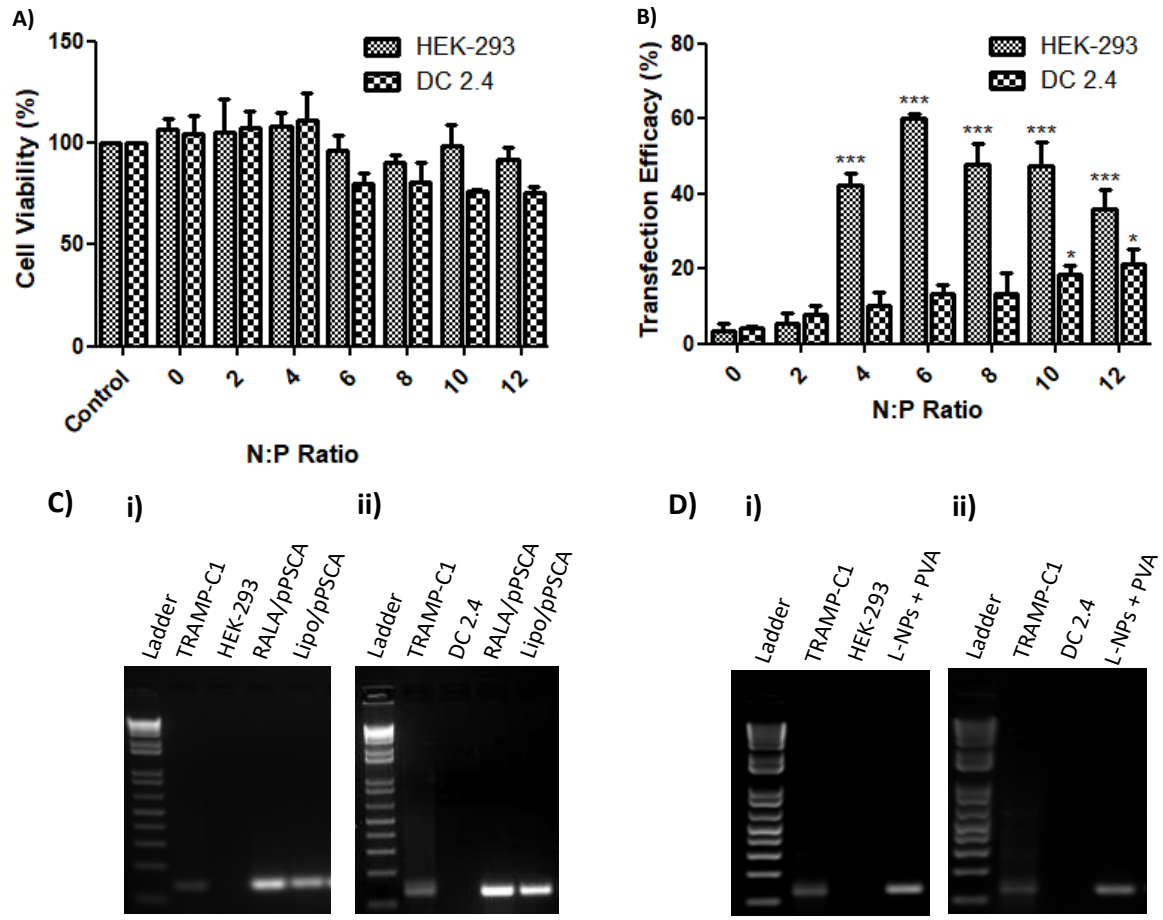

Figure 3: In vitro characterisation of RALA/pPSCA Nanoparticles (NPs). (A) Cytotoxicity analysis and (B) Transfection Efficacy of RALA/pPSCA NPs over a range of N:P ratios (N:P 0-12) in the HEK-293 and DC 2.4 cell lines. (C) Confirmation of PSCA mRNA expression within the i) HEK-293 and ii) DC 2.4 cell lines via reverse transcription (RT)-PCR following transfection of cells with RALA/pPSCA or Lipofectamine/pPSCA complexes. Lane 1: DNA Ladder; Lane 2: TRAMP-C1; Lane 3: untreated HEK-293 or DC 2.4 cells; Lane 4 and 5: HEK-293 or DC 2.4 cells transfected with RALA/pPSCA or Lipofectamine/pPSCA respectively. (D) Confirmation of PSCA mRNA expression within the i) HEK-293 and ii) DC 2.4 cell lines via RT-PCR following transfection of cells with lyophilised RALA/pPSCA (N:P 10) NPs (L-NP) reconstituted and dried in PVA. Lane 1: DNA Ladder; Lane 2: TRAMP-C1; Lane 3: untreated HEK-293 or DC 2.4 cells; Lane 4: : HEK-293 or DC 2.4 cells transfected with L-NPs reconstituted and dried within PVA (L-NPs + PVA).

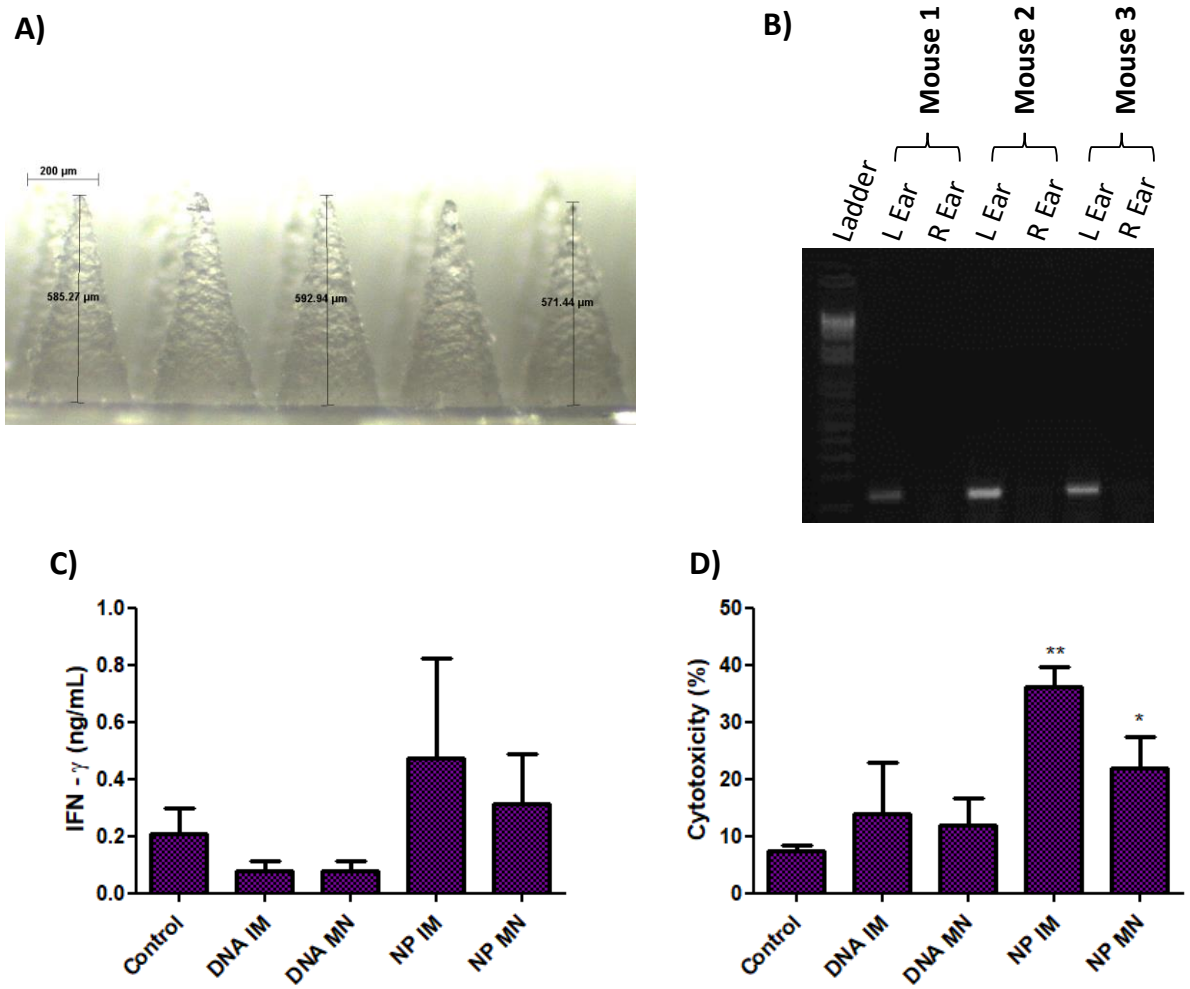

Figure 4: *In vivo* evaluation of PVA microneedles (MNs) loaded with L-NPs (NP-MN). (A) Image of 9-10 kDa PVA MN loaded with L-NPs (NP-MN); (B) Confirmation of PSCA mRNA expression within the right ears of mice treated with NP-MNs encapsulating via RT-PCR. Lane 1: DNA Ladder; Lanes 2, 4 and 6: cDNA from left (L) ears of mice 48 h following application of NP-MN; Lane 3, 5 and 7: cDNA from untreated right (R) ears of mice. (C) Tumour-specific IFN-γ release following stimulation of splenocytes from mice immunised three times at two-weekly intervals with pPSCA (DNA) or RALA/pPSCA (NP) via microneedle (MN) or intramuscular injection (IM). (D) TRAMP-C1 specific toxicity following exposure to stimulated splenocytes from mice immunised as above.

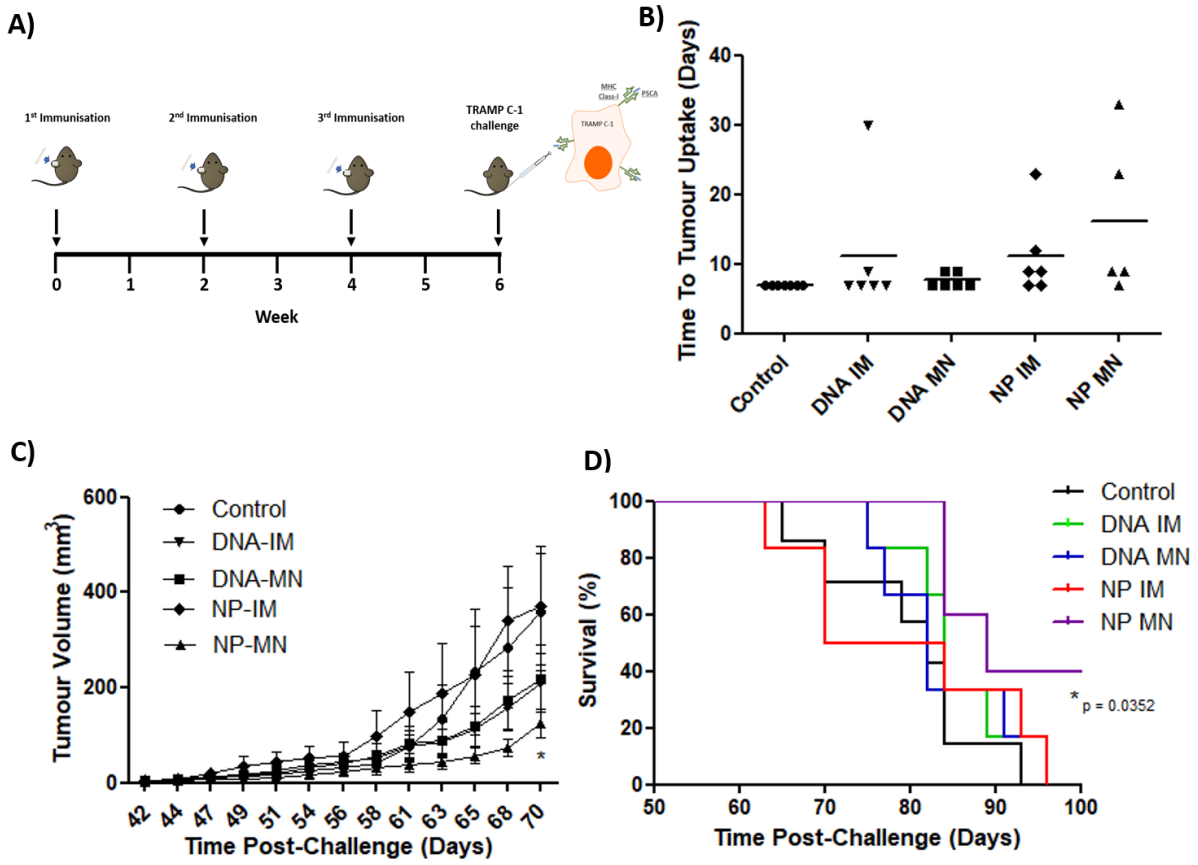

Figure 5: Prophylactic Efficacy of Immunisation with PVA MNs loaded with L-NPs (NP-MN). (A) Schematic of Prophylactic Immunisation Schedule. C57 BL/6 mice were immunised three times at two-weekly intervals with pPSCA (DNA) or RALA/pPSCA (NP) via microneedle (MN) or intramuscular injection (IM). Two weeks following the final immunisation mice were challenged s.c. with $5x10^6$ TRAMP C-1 cells in PBS/Matrigel; (B) Scatter plot of time to tumour formation in immunised mice; (C) Average tumour volume of control and immunised mice; (D) Kaplan-Meier Survival Curve. N = 6/7.

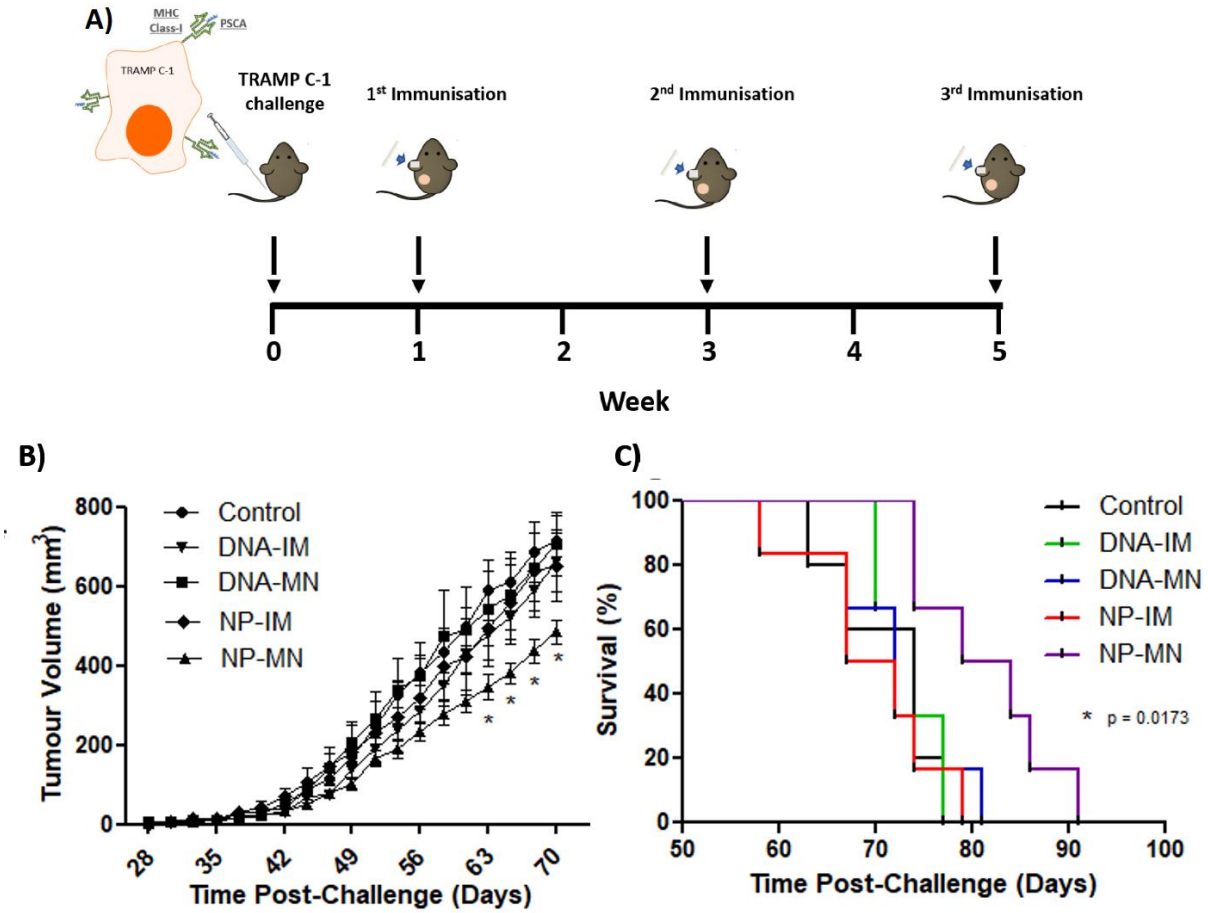

Figure 6: Therapeutic Efficacy of Immunisation with PVA MNs loaded with L-NPs (NP-MN). (A) Schematic of Therapeutic Immunisation Schedule. C57 BL/6 mice were challenged s.c. on the flank with $5x10^6$ TRAMP C-1 cells in PBS/matrigel. One week following tumour challenge mice were immunised three times at two-weekly intervals with DNA-IM, DNA-MN, NP-IM or NP-MN. (B) Average tumour volume of control and immunised mice; (C) Kaplan-Meier Survival Curve. N = 5/6.